Ultrasensitive Surface Plasmon Resonance Detection of Trinitrotoluene by a Bis-aniline-Cross-Linked Au Nanoparticles Composite

Michael Riskin, Ran Tel-Vered, Oleg Lioubashevski, and Itamar Willner*

Institute of Chemistry, The Hebrew University of Jerusalem, Jerusalem 91904, Israel

Received January 11, 2009; E-mail: willnea@vms.huji.ac.il

Abstract: A bis-aniline-cross-linked Au nanoparticles (NPs) composite is electropolymerized on Au surfaces. The association of trinitrotoluene, TNT, to the bis-aniline bridging units via π-donor$-$acceptor interactions allows the amplified detection of TNT by following the surface plasmon resonance (SPR) reflectance changes as a result of the coupling between the localized plasmon of the AuNPs and the surface plasmon wave associated with the gold surface. The detection limit for analyzing TNT by this method is $\sim$10 pM. The electropolymerization of the bis-aniline-cross-linked AuNPs composite in the presence of picric acid results in a molecular-imprinted matrix for the enhanced binding of TNT. The imprinted AuNPs composite enabled the sensing of TNT with a detection limit that corresponded to 10 fM. Analysis of the SPR reflectance changes in the presence of different concentrations of TNT revealed a two-step calibration curve that included the ultrasensitive detection of TNT by the imprinted sites in the composite, $K_{ass.}^{I}$ for the association of TNT to the imprinted sites, 6.4×10^{12} M^{-1}, followed by a less sensitive detection of TNT by the nonimprinted π-donor bis-aniline sites ($K_{ass.}^{NI} = 3.9 \times 10^{9}$ M^{-1}). The imprinted AuNPs composite reveals impressive selectivity. The structural and functional features of the bis-aniline-cross-linked AuNPs composites were characterized by different methods including ellipsometry, AFM, and electrochemical means. The dielectric properties of the AuNPs composite in the presence of different concentrations of TNT were evaluated by the theoretical fitting of the respective experimental SPR curves. The ultrasensitive detection of the TNT by the AuNPs composite was attributed to the changes of the dielectric properties of the composite, as a result of the formation of the π-donor$-$acceptor complexes between TNT and the bis-aniline units. These changes in the dielectric properties lead to a change in the conductivity of the AuNPs matrix.

Introduction

Surface plasmon resonance (SPR) is a versatile tool to probe and detect refractive index changes occurring on metal thin films, e.g., gold films, as a result of chemical events.[1] The assembly of monolayers or thin films on metal surfaces was characterized by SPR spectroscopy,[2] and the method became a widely used tool to monitor biorecognition events on metal surfaces.[3] Numerous studies have applied SPR to develop sensors for analyzing protein$-$protein interactions[4] and to probe the formation of immunocomplexes.[5] The method is, however, hindered by the degree of refractive index changes, which affect the observable changes in the SPR spectra. This requires high-molecular-weight analytes, e.g. proteins that provide sufficient refractive index changes even at a low coverage of the analyte. Different means to enhance the SPR shifts by the conjugation of labels which amplify the refractive index changes, occurring as a result of biorecognition events, were reported, and these include latex particles,[6] liposomes,[7] or secondary proteins[8] as amplifying labels.

Metal nanoparticles (NPs) were also implemented to enhance the SPR response.[9] The coupling between the localized surface plasmon (LSP) of the metal NPs and the surface plasmon polariton (SPP) associated with the thin metal surface leads to a deformation in the dispersion curve of the SPP, and to a shift in the SPR energy. The effects of this coupling were treated theoretically,[9b] and the changes in the SPR curves resulting from the alteration of the dielectric properties of the metal surface

(1) (a) Raether, H. *Surface Plasmons on Smooth and Rough Surfaces and on Gratings, Springer Tracts in Modern Physics*; Springer-Verlag: Berlin, Heidelberg, 1988; Vol. 111. (b) Knoll, W. *Annu. Rev. Phys. Chem.* **1998**, *49*, 569–638.

(2) (a) Ehler, T. T.; Malmberg, N.; Noe, L. J. *J. Phys. Chem. B* **1997**, *101*, 1268–1272. (b) Hutter, E.; Fendler, J. H.; Roy, D. *J. Phys.Chem. B* **2001**, *105*, 11159–11168.

(3) (a) Homola, J. *Chem. Rev.* **2008**, *108*, 462–493. (b) Phillips, K. S.; Cheng, Q. *Anal. Bioanal. Chem.* **2007**, *387*, 1831–1840.

(4) (a) Schuck, P. *Annu. Rev. Biophys. Biomol. Struct.* **1997**, *26*, 541–566. (b) Garland, P. B. Q. *Rev. Biophys.* **1996**, *29*, 91–117. (c) Löfås, S. *Pure Appl. Chem.* **1995**, *67*, 829–834. (d) Heyse, S.; Ernst, O. P.; Dienes, Z.; Hofmann, K. P.; Vogel, H. *Biochemistry* **1998**, *37*, 507–522. (e) Berger, C. E. H.; Beumer, T. A. M.; Kooyman, R. P. H.; Greve, J. *Anal. Chem.* **1998**, *70*, 703–706. (f) Minunni, M. *Anal. Lett.* **1995**, *28*, 933–944.

(5) (a) Fivash, M.; Towler, E. M.; Fisher, R. J. *Curr. Opin. Biotechnol.* **1998**, *9*, 97–101. (b) Malmborg, A. C.; Borrebaeck, C. A. K. *J. Immnunol. Methods* **1995**, *183*, 7–13.

(6) Kubitschko, S.; Spinke, J.; Bruckner, T.; Pohl, S.; Oranth, N. *Anal. Biochem.* **1997**, *253*, 112–122.

(7) Wink, T.; van Zuilen, S.-J.; Bult, A.; van Bennekom, W.-P. *Anal. Chem.* **1998**, *70*, 827–832.

(8) Zayats, M.; Raitman, O. A.; Chegel, V. I.; Kharitonov, A. B.; Willner, I. *Anal. Chem.* **2002**, *74*, 4763–4773.

(9) (a) Lyon, L. A.; Musick, M. D.; Smith, P. C.; Reiss, B. D.; Peña, D. J.; Natan, M. J. *Sens. Actuators, B* **1999**, *54*, 118–124. (b) Agarwal, G. S.; Dutta Gupta, S. *Phys. Rev. B* **1985**, *32*, 3607–3611.

were discussed. Indeed, numerous experiments applied conjugated metallic NPs, mainly AuNPs, as amplifying labels to study biorecognition or biocatalytic events. For example, the formation of immunocomplexes[10] or DNA hybridization[11] were amplified by the conjugation of AuNPs. Also, biocatalytic transformations were enhanced by functionalized AuNPs,[12] and the effects of the particles size[13] and their coverage[13] on the SPR responses were investigated. Specifically, plasmonic coupling between AuNPs aggregates and the surface plasmon wave not only showed shifts of the SPR minimum angle position, but also resulted in a broadening of the resonance curve and in an increase in the minimum reflectance.[14]

Different studies implemented functionalized AuNPs as conjugates that amplify an existing recognition complex. This approach limits, however, the use of the NPs to analyze substrates exhibiting multidentate binding sites. Thus, the use of NPs as amplifying labels for low-molecular-weight substrate is scarce. In the present study we apply a AuNPs composite for the SPR detection of the trinitrotoluene (TNT) explosive. The analysis of TNT attracts recent research efforts due to homeland security needs. Different sensors for analyzing explosives, and particularly, nitroaromatic derivatives were reported in the past decade.[15] These include optical sensors employing functional fluorescent polymers that were quenched by the nitroaromatic explosives,[16,17] luminescent polysilole nanoparticles that were quenched by TNT,[18] or fluorescent silicon nanoparticles that were quenched by nitroaromatic vapors.[19] Furthermore, the electrochemical activity of the nitroaromatic groups was implemented to design modified sensing electrodes, e.g., mesoporous SiO_2 films for electrochemical TNT detection.[20] Other nitroaromatic sensors used the surface acoustic wave readout of the association of TNT to cyclodextrin polymers,[21] carbowax,[22] or silicon polymer[23] matrices deposited on surfaces. Similarly,

competitive immuno-assays were developed for the analysis of TNT. The competitive association of the dye-functionalized TNT and the TNT analyte to anti-TNT-antibody-functionalized quantum dots, and the application of the FRET quenching process were used to develop an optical TNT sensor.[24] Also, the displacement of antigen−anti-TNT antibody complexes linked to surfaces by the TNT analyte was used to develop SPR[25] or microgravimetric quartz crystal microbalance (QCM)[26] antibody-based sensors. In a recent study,[27] we demonstrated the use of thioaniline-modified AuNPs as building units to construct an electropolymerized bis-aniline-cross-linked AuNPs composite on Au electrodes. The cross-linked AuNPs matrix associated with the electrode was used for the electrochemical detection of TNT. π-Donor−acceptor interactions between TNT and the bis-aniline bridges enabled the binding and the concentration of TNT at the electrode surface. Furthermore, we demonstrated the use of the thioaniline-functionalized AuNPs as electropolymerizable units for the generation of specific imprinted sites in the cross-linked AuNPs composite. With the latter tailored nanostructures we were able to detect TNT with a detection limit that corresponded to 200 pM (46 ppt).

Here we report on the highly sensitive detection of trinitrotoluene, TNT (**1**), by a bis-aniline-cross-linked AuNPs matrix associated with a Au-coated glass surface. The formation of the π-donor−acceptor complexes between the TNT and the bis-aniline bridging units is, then, probed by following the effect of these complexes on the plasmon coupling of the AuNPs matrix to the surface plasmon wave. We describe the effect of molecular imprinting of TNT recognition sites into the bis-aniline-cross-linked AuNPs composite on the sensitivity and selectivity of the resulting sensing surface. The bis-aniline-cross-linked AuNPs matrix is characterized by means of electrochemical, AFM, and SPR measurements. Furthermore, by fitting of the experimental SPR curves, we extract the dielectric functions of the sensing matrix upon analyzing TNT. The theoretical fittings of the SPR suggest that the formation of π donor−acceptor complexes between TNT and the bis-aniline units bridging the AuNPs leads to conductivity changes in the NPs composite, and these stimulate the changes in the SPR spectra. Besides the specific application of the bis-aniline-cross-linked AuNPs, composite for the specific analysis of TNT, one may envisage the application of the method for other analytes as well.

Results and Discussion

Thioaniline-functionalized AuNPs, mean diameter 3.5 nm, were prepared by capping the AuNPs with a mixed monolayer of thioaniline (**2**) and mercaptoethane sulfonate (**3**). The resulting functionalized AuNPs were electropolymerized on a thioaniline monolayer-modified flat Au electrode (a glass plate coated with a Au layer, ∼50 nm), by applying 10 electropolymerization cycles ranging between 0.80 to −0.35 V vs Ag/QRE, Scheme 1A. The thickness of the resulting matrix was estimated by ellipsometry measurements to be 9.7 ± 2.1 nm with a volume fraction of AuNPs that equals to approximately 65% ± 19%

(10) (a) Lyon, L. A.; Musick, M. D.; Natan, M. *J. Anal. Chem.* **1998**, *70*, 5177–5183. (b) Mauriz, E.; Calle, A.; Lechuga, L. M.; Quintana, J.; Montoya, A.; Manclus, J. *Anal. Chim. Acta* **2006**, *561*, 40–47.

(11) He, L.; Musick, M. D.; Nicewarner, S. R.; Sallinas, F. G.; Benkovic, S. J.; Natan, M. J.; Keating, C. D. *J. Am. Chem. Soc.* **2000**, *122*, 9071–9077.

(12) Zayats, M.; Pogorelova, S. P.; Kharitonov, A. B.; Lioubashevski, O.; Katz, E.; Willner, I. *Chem.−Eur. J.* **2003**, *9*, 6108–6114.

(13) (a) Lyon, L. A.; Musick, M. D.; Smith, P. C.; Reiss, B. D.; Peña, D. J.; Natan, M. J. *Sens. Actuators, B* **1999**, *54*, 118–124. (b) Lyon, L. A.; Holliway, W. D.; Natan, M. J. *Rev. Sci. Instrum.* **1999**, *70*, 2076–2081. (c) Lyon, L. A.; Peña, D. J.; Natan, M. J. *J. Phys. Chem. B* **1999**, *103*, 5826–5831.

(14) Lyon, L. A.; Peña, D. J.; Natan, M. J. *J. Phys. Chem. B* **1999**, *103*, 5826–5831.

(15) (a) Toal, S. J.; Trogler, W. C. *J. Mater. Chem.* **2006**, *16*, 2871–2883. (b) Senesac, L.; Thundat, T. G. *Mater. Today* **2008**, *11*, 28–36.

(16) (a) Swager, T. M. *Acc. Chem. Res.* **1998**, *31*, 201–207. (b) McQuade, D. T.; Pullen, A. E.; Swager, T. M. *Chem. Rev.* **2000**, *100*, 2537–2574. (c) Yang, J.-S.; Swager, T. M. *J. Am. Chem. Soc.* **1998**, *120*, 11864–11873.

(17) (a) Chang, C.-P.; Chao, C.-Y.; Huang, J.-H.; Li, A.-K.; Hsu, C.-S.; Lin, M.-S.; Hsieh, B.-R.; Su, A.-C. *Synth. Met.* **2004**, *144*, 297–301. (b) Sohn, H.; Sailor, M. J.; Magde, D.; Trogler, W. C. *J. Am. Chem. Soc.* **2003**, *125*, 3821–3830.

(18) Toal, S. J.; Magde, D.; Trogler, W. C. *Chem. Commun.* **2005**, 5465–5467.

(19) Content, S.; Trogler, W. C.; Sailor, M. J. *Chem.−Eur. J.* **2000**, *6*, 2205–2213.

(20) Zhang, H.-X.; Cao, A.-M.; Hu, J.-S.; Wan, L.-J.; Lee, S.-T. *Anal. Chem.* **2006**, *78*, 1967–1971.

(21) Yang, X.; Du, X. X.; Shi, J.; Swanson, B. *Talanta* **2001**, *54*, 439–445.

(22) Kannan, G. K.; Nimal, A. T.; Mittal, U.; Yadava, R. D. S.; Kapoor, J. C. *Sens. Actuators, B* **2004**, *101*, 328–334.

(23) McGill, R. A.; Mlsna, T. E.; Chung, R.; Nguyen, V. K.; Stepnowski, J. *Sens. Actuators, B* **2000**, *65*, 5–9.

(24) Goldman, E. R.; Medintz, I. L.; Whitley, I. L.; Hayhurst, A.; Clapp, A. R.; Uyeda, H. T.; Deschamps, J. R.; Lassman, M. E.; Mattoussi, H. *J. Am. Chem. Soc.* **2005**, *127*, 6744–6751.

(25) Larsson, A.; Angbrant, J.; Ekeroth, J.; Mansson, P.; Liedberg, B. *Sens. Actuators, B* **2006**, *113*, 730–748.

(26) Shankaran, D. R.; Gobi, K. V.; Sakai, T.; Matsumoto, K.; Toko, K.; Miura, N. *Biosens. Bioelectron.* **2005**, *20*, 1750–1756.

(27) Riskin, M.; Tel-Vered, R.; Bourenko, T.; Granot, E.; Willner, I. *J. Am. Chem. Soc.* **2008**, *130*, 9726–9733.

Scheme 1. (A) Electropolymerization of a Bis-aniline-Crosslinked AuNPs Composite for the Sensing of TNT by Donor−Acceptor Interactions; (B) Imprinting of TNT Molecular Recognition Sites into the Bis-aniline-Crosslinked AuNPs Composite Associated with a Au Electrode
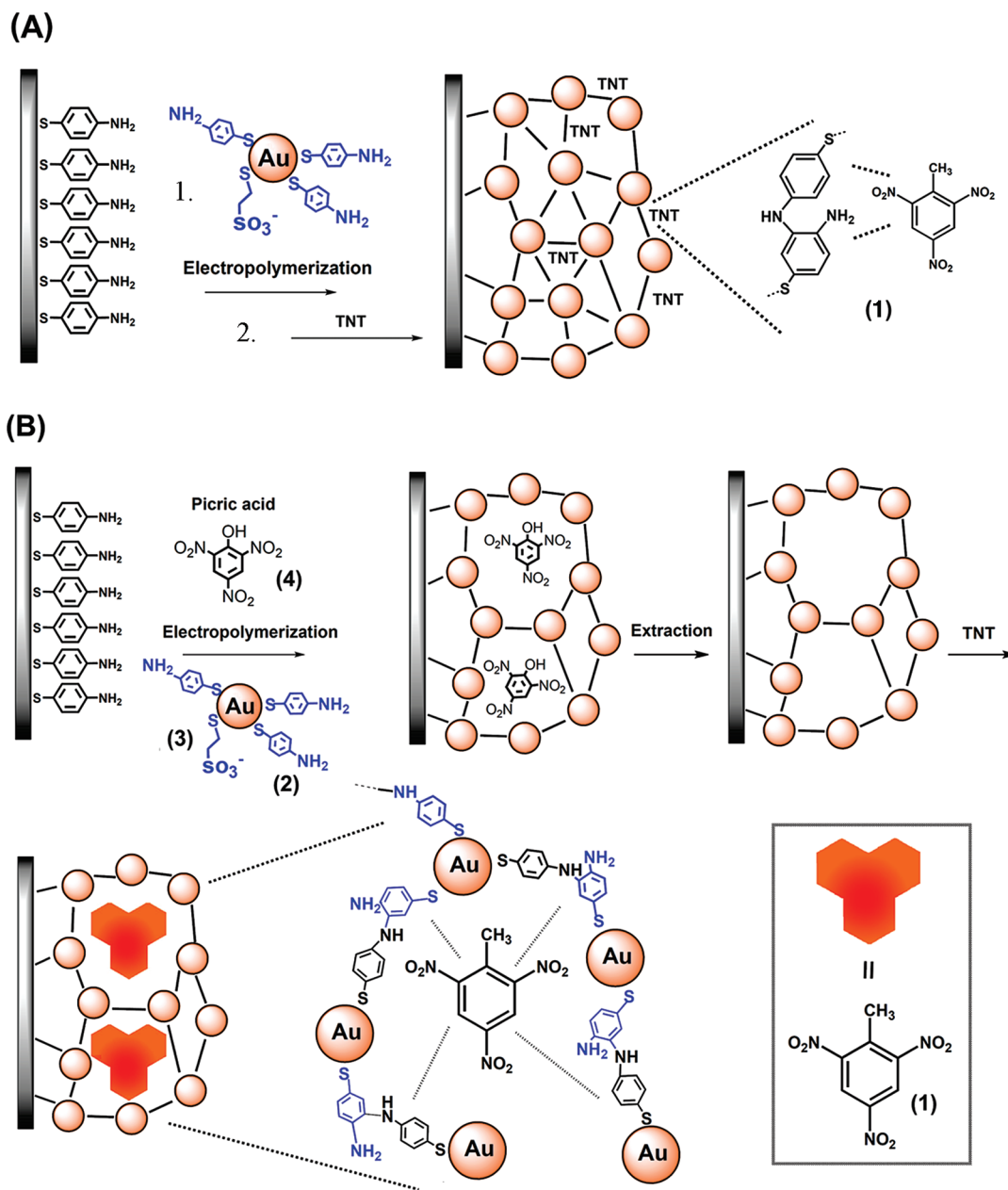
(realizing a 4.5 nm diameter for the AuNPs: 3.5 nm core and 0.5 nm capping shell). This translates to the formation of a AuNPs composite consisting of an average number of approximately three layers (*vide infra*). The bis-aniline cross-linking units exhibit a quasi-reversible redox wave at 0.2 V vs Ag/QRE. Coulometric analysis of the anodic peak corresponding to the bis-aniline units indicated a charge of 6×10^{-5} C·cm^{-2} that translates to a total surface coverage of ~3.8×10^{14} thioaniline molecules·cm^{-2}.

The thioaniline units and bis-aniline bridging units exhibit π-donor properties and, thus, are expected to change the TNT electron acceptor by π-donor−acceptor interactions. The formation of the charge-transfer complex between the bis-aniline π-donor and TNT is, thus, anticipated to alter the dielectric properties of the composite, and this is expected to change the surface plasmon resonance (SPR) features. The change in the dielectric properties at the vicinity of the AuNPs is anticipated

to affect the localized surface plasmon of the AuNPs, and consequently, this will be reflected by the plasmon coupling to the surface plasmon wave. That is, the coupling of the localized plasmon to the surface plasmon is expected to transduce the changes in the dielectric properties of the matrix as a result of the formation of the donor−acceptor complexes.

Figure 1A shows the SPR curve of the bis-aniline-cross-linked AuNPs matrix before interaction with TNT, curve (a), and after interaction with 200 nM of TNT, curve (b). The minimum reflectivity angle of the spectrum is shifted by 0.4°. In a control experiment, a two-layer AuNPs matrix was assembled on the Au-coated glass surface by the primary association of thiopropionic acid-stabilized AuNPs (mean diameter 3.5 nm) on a cystamine-monolayer-functionalized gold slide, followed by the assembly of a second AuNPs layer by cross-linking the AuNPs to the base AuNPs layer with butane dithiol. Interaction of this AuNPs matrix with TNT, 200 nM, did not yield any significant
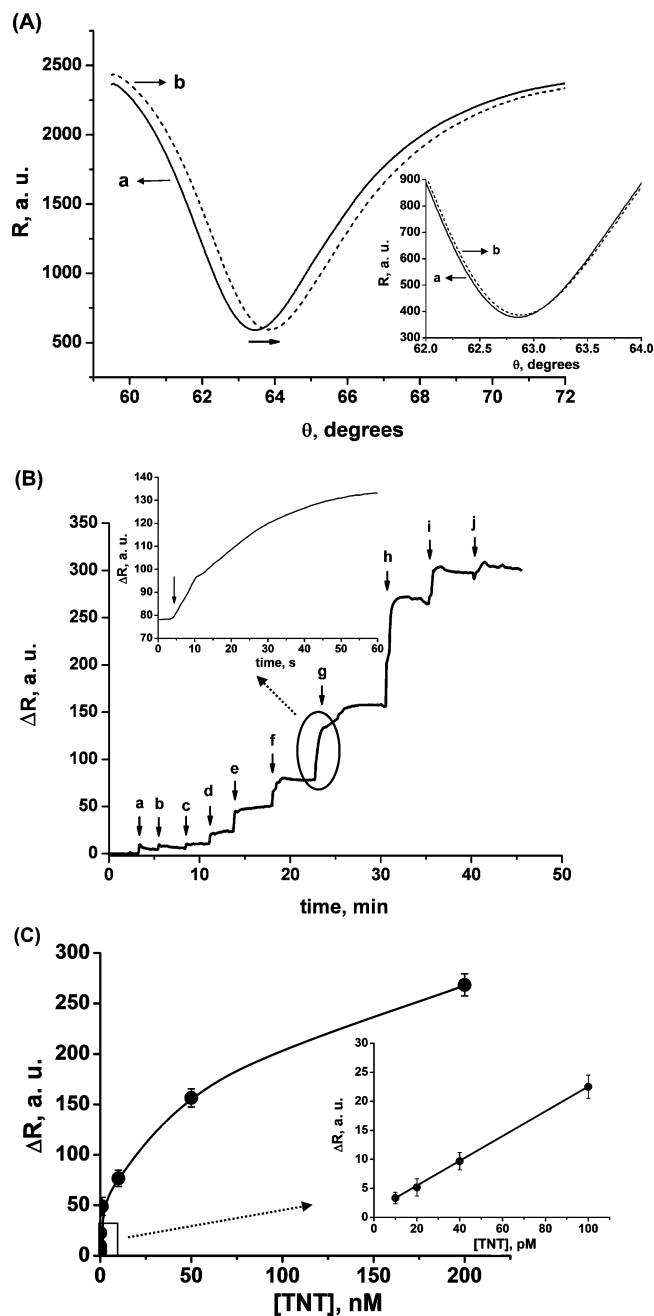
Figure 1. (A) SPR curves corresponding to the bis-aniline-AuNPs composite: (a) before the addition of TNT and (b) after the addition of TNT, 200 nM. Inset: SPR curves corresponding to a bilayer of AuNPs cross-linked by 1,4-butane dithiol and linked to the cystamine-modifed Au surface: (a) before, and, (b) after the addition of TNT, 200 nM. (B) Sensogram corresponding to the changes in the reflectance intensities, at $\theta = 62.4°$, upon addition of variable concentrations of TNT: (a) 10 pM, (b) 20 pM, (c) 40 pM, (d) 100 pM, (e) 1 nM, (f) 10 nM, (g) 50 nM, (h) 200 nM, (i) 1 μM, (j) 5 μM. Arrows indicate the time of addition of the analyte. Inset: enlarged time-dependent reflectance changes. (C) Calibration curve relating the reflectance changes to the concentration of TNT. Inset: responses in low concentration range. All measurements were performed in a 0.1 M HEPES buffer solution, pH = 7.2.

change in the SPR spectrum of the surface (Figure 1A, inset), and only upon the interaction of the surface with 1 μM TNT, was a minute shift in the SPR spectrum observed. Thus, when the bridging units lack electron-donating properties, the SPR spectrum of the system is almost unaffected by the addition of TNT. This is consistent with the primary assumption that the

association of TNT to the AuNPs surface occurs only upon the formation of π-donor–acceptor complexes between the bis-aniline units and TNT (for further supporting evidence, *vide infra*). In a further control experiment polyaniline was electropolymerized on a Au-coated glass surface, and the SPR curves of the film were recorded before and after interaction with TNT, 200 nM. The measurements indicated no changes in the SPR spectrum of the film in the presence of TNT. This implies that the changes in the SPR spectrum of the AuNPs composite upon the association of TNT are amplified through the coupling of the localized plasmon of the NPs with the surface plasmon wave. Figure 1B shows the sensogram corresponding to the reflectance changes, ΔR, upon the treatment of the bis-aniline-cross-linked AuNPs matrix with variable concentrations of TNT, and Figure 1C depicts the corresponding calibration curve derived from the reflectance changes at $\theta = 62.4°$, upon the bis-aniline-cross-linked AuNPs-modified electrode interaction with variable concentrations of TNT. The time-response of the sensing device is ~1 min, Figure 1B, inset. The modified electrode enables the detection of TNT with a detection limit corresponding to ~10 pM (signal/noise (S/N) = 5).

We searched, however, to improve the sensitivity of the analysis of TNT. Any method to enhance the binding affinity of TNT to the sensing matrix is anticipated to lead to improved sensitivities. In a previous report,[27] we implemented the molecular imprinting principle to generate TNT binding sites by the electropolymerization of the AuNPs under conditions that yielded imprinted sites with enhanced binding affinities for TNT. According to this method, Scheme 1 B, the thioaniline-functionalized AuNPs act as electropolymerizable nanometer-sized units for generating the imprinted sites, and picric acid (**4**) serves as an analogue for TNT and is used for the imprinting process. Formation of the π-donor–acceptor complexes between the picric acid and the thioaniline-modified AuNPs occurs during the electropolymerization on the Au-coated slide. The subsequent removal of the picric acid imprint molecules yields molecular contours with optimal positioning of the π-donor sites for the association of the TNT analyte. Indeed, in the previous study[27] it was demonstrated that the synergistic binding of TNT to the AuNPs matrix by π-donor–acceptor interactions and molecular contours improved the association constant of TNT to the matrix. Figure 2A depicts the SPR curve of the imprinted cross-linked AuNPs composite before, curve (a), and after treatment with 1 pM of TNT, curve (b). The SPR shift at this low concentration is comparable to the response of the nonimprinted matrix at 200 nM TNT, Figure 1A, indicating that an increased coverage of TNT on the sensing surface occurred. Figure 2B depicts the reflectance changes at the angle $\theta = 62.7°$, upon treating the imprinted sensing matrix with variable concentrations of TNT. As the concentration of TNT is elevated, the reflectance changes increase. Figure 2C shows the derived calibration curve that corresponds to the analysis of TNT by the imprinted matrix. The detection limit for the analysis of TNT using the imprinted composite corresponds to a concentration of 10 fM TNT (S/N = 5, the response time for the TNT analysis is ~15 s., Figure 2B, inset) that is ~10^3-fold improved relative to the nonimprinted matrix. Figure 3, depicts the comparison of the derived calibration curves for the imprinted, curve (a), and the nonimprinted, curve (b), matrices, presented for clarity on a semilogarithmic scale. The enhanced SPR shifts and the improved sensitivity for the detection of TNT by the imprinted bis-aniline-cross-linked AuNPs matrix are attributed
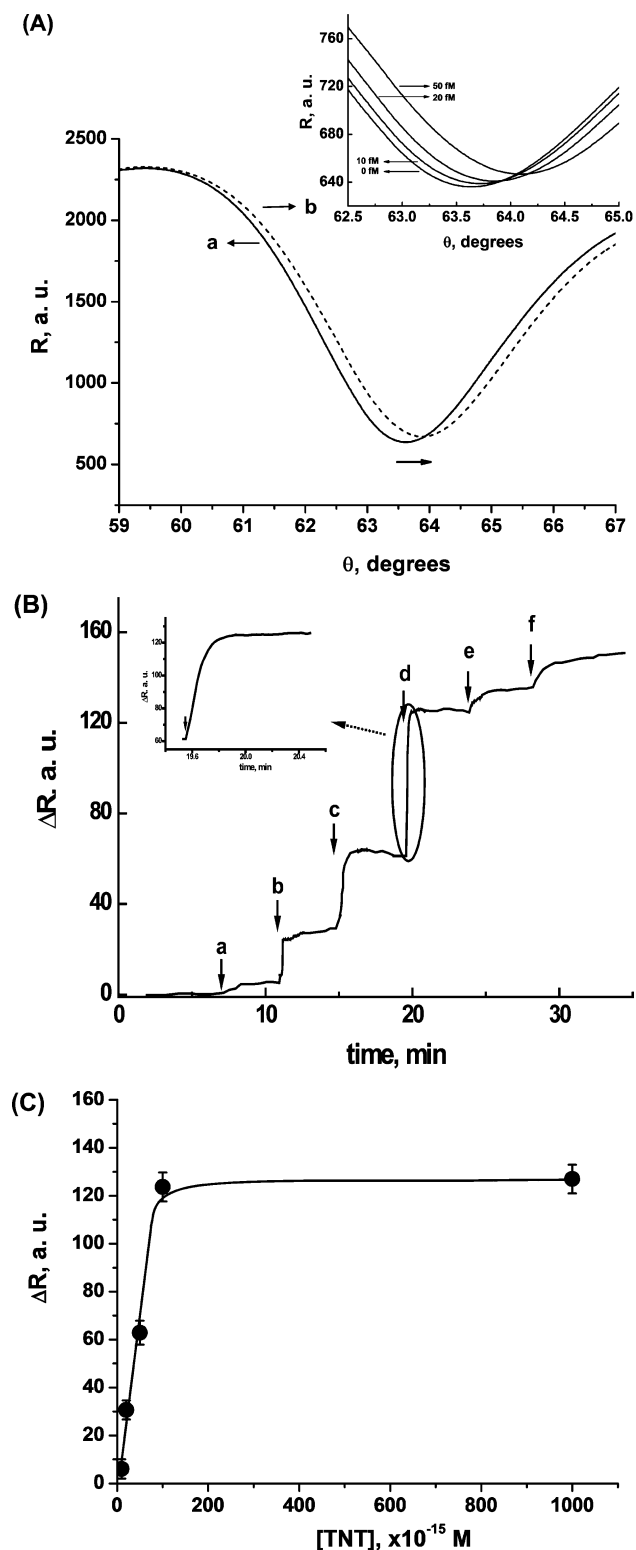
Figure 2. (A) SPR curves corresponding to the picric acid-imprinted bis-aniline-AuNPs composite: (a) before the addition of TNT, and (b) after the addition of TNT, 1 pM. Inset: SPR curves (enlarged at the minimum reflectance angle) corresponding to the picric acid-imprinted bis-aniline-AuNPs composite in the presence of different concentrations of TNT. (B) Sensogram corresponding to the changes in the reflectance intensities, at θ = 62.4°, upon addition of variable concentrations of TNT: (a) 10 fM, (b) 20 fM, (c) 50 fM, (d) 100 fM, (e) 1 pM, (f) 5 pM. Arrows indicate the time of addition of the analyte. Inset: enlarged time-dependent reflectance changes. (C) Calibration curve relating the reflectance changes to the concentration of TNT. All measurements were performed in a 0.1 M HEPES buffer solution, pH = 7.2.
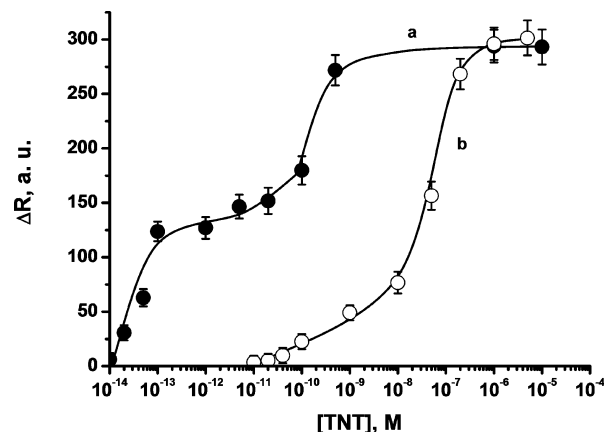
Figure 3. Changes in the reflectance intensities upon analyzing TNT within a broad range of concentrations (presented on a semilogarithmic scale): (a) Imprinted bis-aniline-cross-linked AuNPs composite. (b) Nonimprinted bis-aniline-cross-linked AuNPs composite. All measurements were performed in a 0.1 M HEPES buffer solution, pH = 7.2.

to the higher affinity of TNT to the imprinted matrix, resulting in higher content of bound TNT (*vide infra*).

One may note that for the imprinted AuNPs composite two steps of changes in the reflectance values as a function of the concentration of added TNT, are observed. The first step is initiated at ~10 fM TNT, and the reflectance change (ΔR) saturates at ~5 pM. The second step of reflectance change is initiated at ~100 pM and the reflectance levels off at ~1 nM. In contrast, the nonimprinted matrix shows a single domain of ΔR that is initiated at ~10 pM and it reaches a saturation value at ~1 μM. The two-step reflectance calibration curve, Figure 3, curve (a), is attributed to the existence of two types of TNT binding sites. The reflectance changes at low TNT concentrations (10 fM < [TNT] < 5 pM) are attributed to the association of TNT to the imprinted donor sites of the matrix. The reflectance changes observed at higher TNT concentrations (100 pM < [TNT] < 10 μM) that are also observed for the nonimprinted matrix are attributed to the association of TNT to the nonimprinted bis-aniline π-donor units. It should be noted that the inflection point of the second step for analyzing TNT by imprinted Au NPs matrix in Figure 3, curve (a), occurs at a concentration that is ~2 orders of magnitude lower than the inflection point for the analysis by the nonimprinted Au NPs matrix, curve (b). This presumably originates from the fact that the imprinting process leads to nonoptimal, partially fitting binding sites for TNT molecules. The association constant to these sites is still higher than to the nonimprinted bridging units, leading to the inflection point at a lower concentration. Also, the imprinted Au NPs composite and the nonimprinted one reach similar saturation reflectance changes. This is consistent with the fact that the content of bis-aniline bridging units in both composites is similar. The only difference between the composites is that a fraction of the bis-aniline binding sites participated in structurally imprinted domains that revealed enhanced binding toward TNT.

The specificity of the picric acid-imprinted polymer matrices toward the analysis of TNT was further examined by subjecting the imprinted AuNPs composite to 2,4-dinitrotoluene (DNT), **5**. Figure 4A depicts the comparison between the calibration curves derived for TNT, curve (a), and DNT, curve (b). While the interaction of the imprinted matrix yields detectable reflectance changes with a bulk TNT concentration of 10 fM,
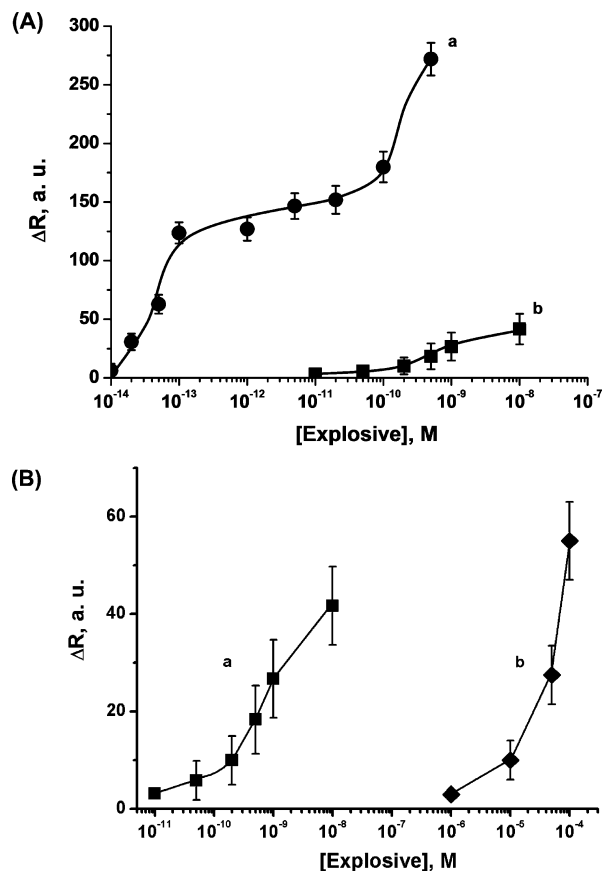
Figure 4. (A) Calibration curves (presented on a semilogarithmic scale) corresponding to the analysis of: (a) TNT, and (b) 2,4-dinitrotoluene by the imprinted bis-aniline-cross-linked AuNPs composite. (B) Calibration curves (presented on a semilogarithmic scale) corresponding to the analysis of: (a) 2,4-dinitrotoluene, and (b) 4-nitrotoluene, by the imprinted bis-aniline-cross-linked AuNPs composite. All measurements were performed in a 0.1 M HEPES buffer solution, pH = 7.2.

Figure 5. Effect of applied potential on the reflectance changes, at $\theta = 62.4°$, of the bis-aniline-cross-linked AuNPs composite, upon analyzing TNT, 100 fM: (a) the imprinted composite and (b) the nonimprinted composite. All measurements were performed in a 0.1 M HEPES buffer solution, pH = 7.2.

comparable ΔR values for DNT are observed only at bulk concentrations above 50 pM. Also, the saturation values of ΔR for TNT sensing ($\Delta R \sim 300$ au) are substantially higher than ΔR upon sensing of DNT ($\Delta R \sim 40$ au). These results are consistent with the fact that DNT exhibits substantially lower affinity toward the picric acid-imprinted matrix, as compared to TNT. The lower affinity of DNT to the imprinted matrix defines the lower content of DNT associated with the matrix, resulting in a substantially higher detection limit and a lower response.

While the imprinted AuNPs matrices sense TNT in the femtomolar concentration range, these matrices respond to DNT only in the picomolar concentration range. That is, the analysis of TNT by the imprinted AuNPs matrix is $\sim 10^3$-fold more sensitive than the detection of DNT. This result is consistent with the fact that DNT exhibits decreased electron-acceptor properties as compared to TNT due to the lack of one of the electron-attracting nitro groups. The lower electron affinity of DNT results in a weaker binding constant with the π-donor cross-linking units, and thus, higher bulk concentrations are needed to yield a measurable SPR response. These conclusions are even further emphasized upon the analysis of 4-nitrotoluene (MNT), **6**, Figure 4B. The detection limit for analyzing mononitrotoluene, MNT is in the 10^{-5} M concentration range only, and no difference is observed upon sensing MNT by the
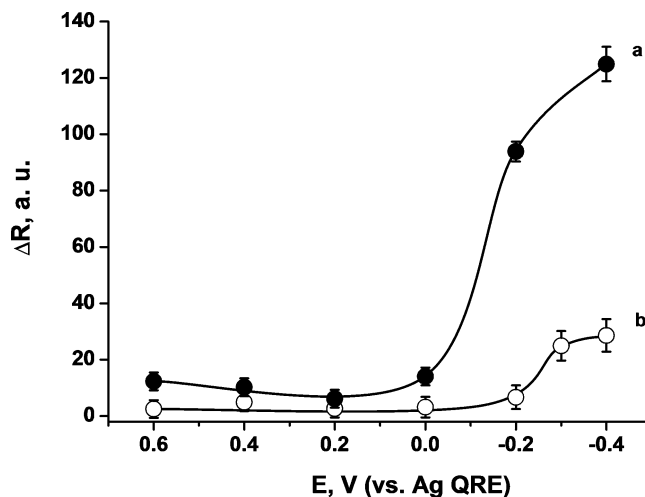
imprinted or nonimprinted matrices. Evidently, the lack of two of the electron-withdrawing NO_2 groups weakens the electron-acceptor features of MNT as compared to TNT and DNT, and thus, higher bulk concentrations of MNT are required to allow their association to the π-donor sites. It should be noted that the selectivity does not originate only from the π-donor−acceptor interactions of the explosives with the matrix but is also controlled by the steric fitting of the explosive molecules to the imprinted sites. For example, trinitrotriazine (RDX), exhibiting similar electron-acceptor features to those of TNT, is not sensed by the picric acid-imprinted composite below the nanomolar region, due to the larger dimensions of the RDX molecules.

Further support that the successful ultrasensitive detection of TNT originates, indeed, from π-donor−acceptor interactions with the bis-aniline bridges was obtained by following the SPR changes in reflectance, ΔR, of the imprinted, or nonimprinted, AuNPs cross-linked composites in the presence of TNT (100 fM), upon applying an external potential on the Au surface, Figure 5, curves (a) and (b), respectively. A sharp change in the SPR reflectance intensities is observed at ~ -0.1 V (vs a quasi-reversible Ag wire reference electrode). Prior to the addition of TNT, the potential scan of the electrode revealed only a minute reflectance change in the entire potential range, specifically, at -0.1 V vs the Ag wire electrode, (<5 au of reflectance). These results further support the formation of the π-donor−acceptor complexes in the bis-aniline-cross-linked AuNPs composite, and re-emphasize that the charge transfer process in the donor−acceptor complexes strongly affects the SPR spectra. In the potential region of +0.6 to 0.0 V, the bridging units exist in their oxidized, quinoide, form. In this state, the bridges exhibit electron-acceptor features, and thus, the formation of the donor−acceptor complexes with TNT is prohibited. At the potential of ~ -0.1 V, the bridging units are reduced to the bis-aniline π-donor form. In this configuration, the formation of the π-donor−acceptor complex with TNT proceeds, resulting in the changes in the SPR spectra. The increased changes in the reflectance intensities observed for the imprinted cross-linked AuNPs composite (cf. Figure 5, curve

(a) as compared to (b)) are consistent with the enhanced binding of TNT to the imprinted sites.

Further attempts were directed to characterize the structure and composition of the bis-aniline-bridged AuNPs matrix. Ellipsometry was implemented as a spectroscopic tool. Ellipsometry is a powerful optical technique for the investigation of the dielectric properties of thin films,[28] and it has been widely used to characterize polymer layers and NP−polymer composites.[29] In ellipsometric measurements the incident polarized monochromatic light beam is reflected from the sample. The reflected beam intensity and polarization changes are then measured, yielding the ellipsometric angles Ψ and Δ. These experimental quantities are compared with the values calculated according to the suggested model describing the order of the layers on the surface, and a least-squares value minimization is performed. The optical properties of 2−4 nm diameter AuNPs were recently studied through optical absorption and ellipsometric measurements, and their dielectric function was found to be nearly equal to that of bulk gold in the spectral range of 207−414 nm.[30] These observations allowed us to integrate the optical properties of bulk gold in the ellipsometric model for the characterization of the electropolymerized AuNP matrices by fitting the ellipsometric data in the spectral range of 300−500 nm. By analyzing the ellipsometry results, we estimated the thickness of the thioaniline monolayer to be 1.1 ± 0.2 nm, using a refractive index of $n = 1.56$ for thioaniline.[31] The thickness of the bis-aniline-cross-linked AuNPs matrix was estimated by using the effective medium approximation, based on the Maxwell−Garnett approach that describes the relationship between the effective dielectric function of the composite and the dielectric function and volume fraction of the metallic NPs. We used a model that included a composite consisting of gold spheres embedded in a thioaniline linker medium containing voids. The estimated thickness of the cross-linked AuNPs composite was found to be 9.7 ± 2.1 nm with a volume fraction of AuNPs corresponding to ∼65 ± 19%. This value translates to a surface coverage of ∼1.3 × 10^13 NPs·cm^−2. Using the measured dimensions of the AuNPs (4.5 nm, including the capping shell), this thickness translates to approximately three monolayers of AuNPs in the matrix. Further characterization of the composite was accomplished by electrochemical measurements. The AuNPs were synthesized with a molar ratio of thioaniline/ethane-sulfonic acid mixture (mercaptoethane sulfonate) that corresponded to 1:6. It was previously estimated[32] that ∼220 thiol molecules bind to a single AuNP with a core size of 4.0 nm. This value was recalculated for the 3.5 nm AuNPs used in the present study, to yield a coverage of ∼170 thiol molecules per single AuNP. Realizing that thioaniline provides only 1/7 of the total coverage, we estimated that a single AuNP is covered by ∼25 thioaniline units.

The amount of the thioaniline units, electropolymerized in the AuNP composite, was further probed by the coulometric analysis of the cathodic redox wave at 0.05 V vs SCE. The charge associated with the oxidation of the thioaniline units corresponded to 6×10^{-5} C·cm^−2, a value that translates to a coverage of 3.8×10^{14} thioanilne molecules·cm^−2 in the composite. Realizing that each AuNP is covered by 24 thioaniline units, we estimate the surface coverage of the AuNPs to be 1.6×10^{13} particles·cm^−2. Using the derived surface coverage of the AuNPs, and knowing the volume of a single AuNP, we estimate the thickness of the composite to be ∼11.6 nm, assuming a random close packing model for the AuNPs in the matrix.[33] This result suggests that the composite consists of approximately three random densely packed AuNPs layers, consistent with the ellipsometry results. It should be noted that the ellipsometric and the electrochemical methods yielded similar surface coverage values of the AuNPs.

We then evaluated the association constant of TNT binding to the bis-aniline-AuNPs units in the imprinted matrix and the content of imprinted sites in the matrix to estimate the relative population of the sites bound by TNT. The binding of TNT to the π-donor binding sites in the imprinted and nonimprinted AuNPs matrices can be described by eq 1 and the Langmuir isotherm model.[34] According to this model, the association constant of TNT to the π-donor binding sites, is given by eq 2 where θ is the number of sites occupied by TNT, and α is the total number of binding sites. At any given bulk concentration of TNT, the value of θ can be evaluated by rearranging eq 2 in the form of eq 2a.

$$\text{TNT} + \pi\text{-donor sites} \rightleftharpoons \text{TNT-bound sites} \quad (1)$$
$$\alpha\text{-}\theta \qquad \theta$$
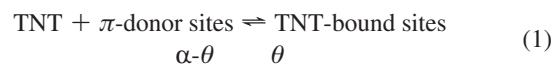
$$K_{\text{ass.}} = \frac{\theta}{(\alpha - \theta)[\text{TNT}]} \quad (2)$$

or

$$\theta = \frac{\alpha K_{\text{ass.}}[\text{TNT}]}{1 + K_{\text{ass.}}[\text{TNT}]} \quad (2a)$$

The double reciprocal of the Langmuir equation yields the Lineweaver−Burk relation, eq 3:

$$\frac{1}{\theta} = \frac{1}{\alpha} + \frac{1}{\alpha K_{\text{ass.}}[\text{TNT}]} \quad (3)$$

From the values of the slope and the y-axis intercept the values of α and $K_{\text{ass.}}$ can then be derived. Assuming that the reflectivity, R, is proportional to the number of TNT-occupied sites, θ, we analyzed the calibration curves for the nonimprinted and the imprinted matrices, Figures 1C and 2C, respectively, according to the Lineweaver−Burk relation, eq 3. The derived association constants for the imprinted and the nonimprinted sites correspond to, $K_{\text{ass.}}^{\text{I}} = 6.4 \times 10^{12}$ M^−1, and $K_{\text{ass.}}^{\text{NI}} = 3.9 \times 10^9$ M^−1, respectively.

Figure 3 presents the calibration curves derived for the imprinted and nonimprinted matrices on a semilogarithmic scale. One can realize a two-step sensing response in the calibration curve for the imprinted matrix. We believe that this behavior is defined by two populations of binding sites which possess

(28) Tompkins, H. G. *A Users's Guide to Ellipsometry*; Academic Press Inc; London, 1993.

(29) (a) Kurbitz, S.; Porstendorfer, J.; Berg, K.-J.; Berg, G. *Appl. Phys. B - Lasers and Optics* 2001, *73*, 333–337. (b) Okamura, M.; Kondo, T.; Uosaki, K. *J. Phys. Chem. B* 2005, *109*, 9897–9904. (c) Schelm, S.; Smith, G.-B.; Wei, G. *Nano Lett.* 2004, *4*, 335–339.

(30) Palpant, B.; Prevel, B.; Lerme, J.; Cottancin, E.; Pellarin, M.; Treilleux, M.; Perez, A.; Vialle, J. V.; Broyer, M. *Phys. Rev. B* 1998, *57*, 1963–1970.

(31) Okamura, M.; Kondo, T.; Uosaki, K. *J. Phys. Chem. B* 2005, *109*, 9897–9904.

(32) Hostetler, M. J.; Wingate, J. E.; Zhong, C. J.; Harris, J. E.; Vachet, R. W.; Clark, M. R.; Londono, J. D.; Green, S. J.; Stokes, J. J.; Wignall, G. D.; Glish, G. L.; Porter, M. D.; Evans, N. D.; Murray, R. W. *Langmuir* 1998, *14*, 17–30.

(33) We assume a AuNPs volume filling coefficient of 0.64, in accordance with a random close packing model, and use a AuNP diameter that equals to 4.5 nm (3.5 nm mean core diameter with a 0.5 nm capping layer).

(34) Mazel, R. *Principles of Adsorption and Reaction on Solid Surfaces*; Wiley Interscience: New York, 1996; Vol. 240.
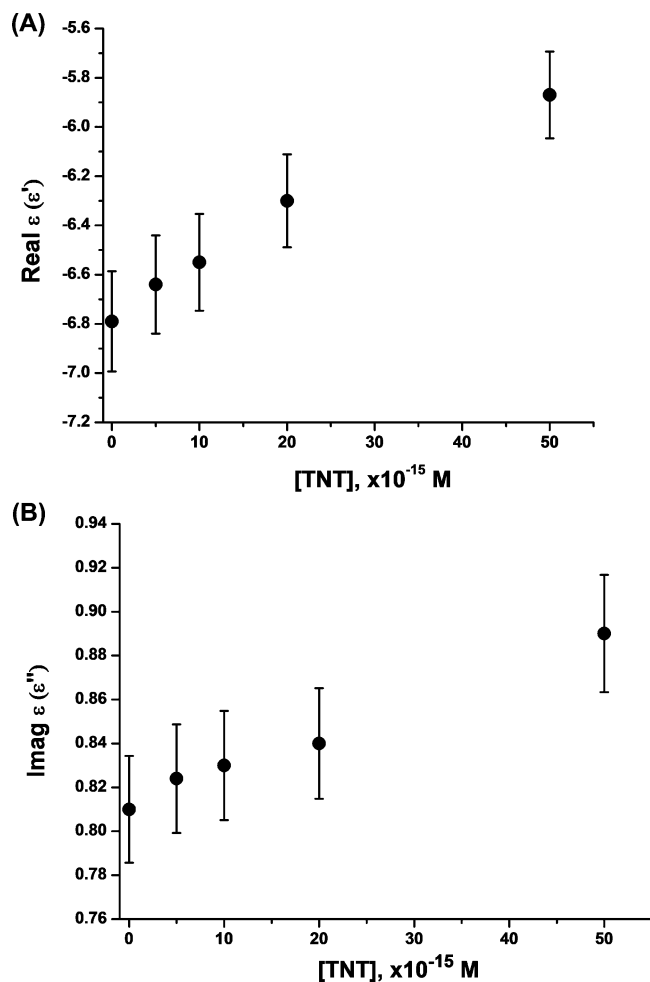
Figure 6. (A) Calculated changes in the real-part of the dielectric constant of the imprinted bis-aniline-cross-linked AuNPs composite upon analyzing different concentrations of TNT. (B) Calculated changes in the imaginary part of the dielectric constant of the imprinted bis-aniline-cross-linked AuNPs composite upon analyzing different concentrations of TNT.
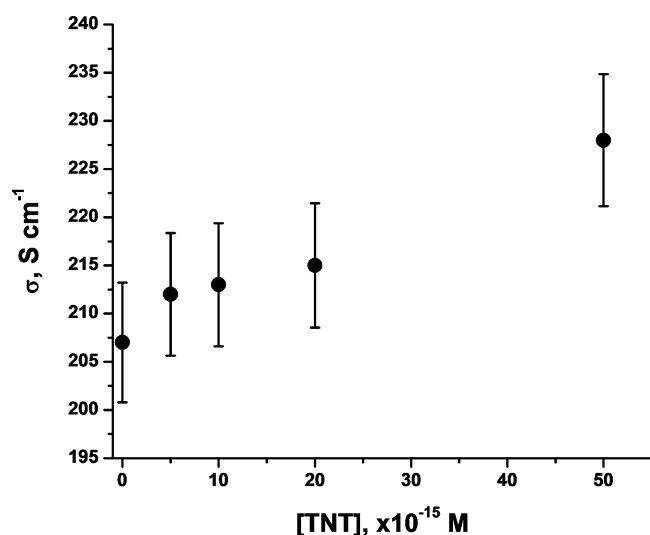

Figure 7. Calculated conductivity of the imprinted bis-aniline-cross-linked AuNPs composite upon analyzing different concentrations of TNT.

different association constants for TNT binding, and correspond to the association to the imprinted and nonimprinted sites in

the imprinted matrix. We use the Langmuir model for these two populations in order to describe the experimentally derived calibration curve. Assuming that the imprinted AuNPs matrix includes only two types of sites, imprinted and nonimprinted, then each of the independent sites binds TNT according to eq 3, and the relation describing the coverage of TNT in these two types of sites is given by eq 4:

$$\theta = \frac{\alpha_1 K_{\text{ass.}}^{\text{I}}[\text{TNT}]}{1 + K_{\text{ass.}}^{\text{I}}[\text{TNT}]} + \frac{\alpha_2 K_{\text{ass.}}^{\text{NI}}[\text{TNT}]}{1 + K_{\text{ass.}}^{\text{NI}}[\text{TNT}]} \quad (4)$$

The experimental calibration curve was then fitted to eq 4, allowing the extraction of $K_{\text{ass.}}^{\text{I}} = 1.7 \times 10^{13}$ M^{-1} and $K_{\text{ass.}}^{\text{NI}} = 5.4 \times 10^{9}$ M^{-1}, which correspond to the association constants of TNT to the imprinted and nonimprinted sites, respectively. Also, the analysis indicated that the relative fraction of imprinted sites is ~48% of the total number of binding sites in the matrix. Evidently, both the Lineweaver−Burk analysis and the two population fitting methods resulted in close values for each of the association constants between TNT and the two types of binding sites associated with the sensing matrix.

The lowest SPR detectable concentration of TNT by the imprinted AuNPs matrix corresponded to 10 fM. Substitution of the derived values of association constants $K_{\text{ass.}}^{\text{I}}$ and $K_{\text{ass.}}^{\text{NI}}$ (derived from the calibration curves) into eq 4 yields the relative coverage of the TNT occupied sites, θ/α, ~ 4.7%. Thus, at the lowest concentration detected, less than 5% of the total number of binding sites are occupied. In order to understand the effects of bound TNT on the SPR shifts and particularly to realize the effect of the low detectable concentrations of TNT on the SPR changes, we analyzed the experimental curves. The SPR curve is characterized by three major values: θ_p, Γ_w, and R_{min}, where θ_p and R_{min} correspond to the minimum reflectivity plasmon angle and the reflectance at this angle, respectively, and Γ_w is the width of the SPR curve at half of the maximum reflectance intensity. The experimental results reveal that the binding of TNT results in changes in R_{min}, θ_p, and Γ_w. Accordingly, we fitted the different SPR spectra in a reduced range of SPR angles (±1.5° around the plasmon angle), by using Frenel's equations-based five-layer model in the Winspall 2.0 program. The derived values for the real and imaginary parts of the complex index of refraction $n = n_R + ik$ for the different curves were, then, translated into the real and imaginary parts of the complex dielectric constant values, ε' and ε'', respectively. Equation 5 relates the complex index of refraction to the complex dielectric function, $\varepsilon = \varepsilon' + \varepsilon''$.

$$\varepsilon = n^2 \quad (5)$$

$$\varepsilon' = n_R^2 - k^2 \quad (5a)$$

$$\varepsilon'' = 2n_R k \quad (5b)$$

The results for the fitting of the SPR curves corresponding to the Au layer-coated SPR slide, the thioaniline monolayer-modified surface, the surface after the stepwise deposition of the bis-aniline-bridged AuNPs composite, and the modified surface treated with variable concentrations of TNT are summarized in Table 1. The values of the dielectric constants for the Au-coated SPR slide are very close to the reported values for bulk gold[35] ($\varepsilon' = -13.4$; $\varepsilon'' = 1.4$) and provide a further support for the fitting procedure. Parts A and B of Figure 6

(35) Palik, E. D., Ed. *Handbook of Optical Constants of Solids III*; Academic Press: New York, 1998.

Table 1. Parameters Derived by Fitting the Experimental SPR Curves

	d, nm	*n*	*k*	*ε′*	*ε″*	*σ*, S·cm^{-1}
bare Au/Cr	54.3	0.186	3.91	−13.92	1.39	
thioaniline SAM	1.29	1.68	0	2.82		
AuNPs matrix	7.03	0.1546	2.61	−6.79	0.81	207
TNT 5 fM		0.1601	2.58	−6.64	0.824	212
TNT 10 fM		0.1616	2.57	−6.60	0.83	213
TNT 20 fM		0.1665	2.52	−6.30	0.84	215
TNT 50 fM		0.1834	2.43	−5.87	0.89	228

depict the calculated values of the real part, *ε′*, and of the imaginary part, *ε″*, respectively, of the dielectric constant associated with the bis-aniline-cross-linked AuNPs matrix in the presence of variable concentrations of TNT. The values of the dielectric constant components are smaller than those of bulk Au[36] and are strongly affected by the association of TNT with the formation of the respective donor−acceptor complexes. The real part of the dielectric constant, *ε′*, for the AuNPs exhibits values that are 2-fold lower than the corresponding value for bulk gold. Upon the increase of the TNT concentration and the formation of the respective π-donor−acceptor complexes the real part of the dielectric constant increases and becomes less negative. The same tendency is observed for the imaginary part of the dielectric constant, *ε″*, that increases as the coverage of TNT is elevated. For example, at a bulk TNT concentration of 50 fM, *ε″* increases by 10%. The changes in *ε″* are possibly connected to the electrical conductivity of the bis-aniline-AuNPs matrix. According to the semiclassical Drude model for metal-like conductor, the electrical conductivity in the optical frequencies range is coupled to its optical properties.[36] The conducting material is characterized by the complex dielectric function, *ε*, and in the presence of an incident light of wavelength *λ*, the conductivity, *σ*, is given by eq 6, where *ε″* is the imaginary part of the dielectric constant, *c* is the speed of light, and *ε₀* is the free-space permittivity.

$$\varepsilon'' = i2\sigma\lambda/c\varepsilon_0 \qquad (6)$$

It can be seen from this equation, that a variation of the conductivity of the layer can cause a change in the imaginary part of the dielectric constant. The fitting of the SPR curves, upon the association of TNT, revealed that the imaginary part of the dielectric constant increases as the TNT concentration is elevated. This implies that the conductivity of the AuNPs matrix increases, too, as the coverage of TNT becomes higher. Figure 7 presents the calculated values of the conductivity changes as a function of the TNT concentration. Our analysis suggests that the electrical conductivity of the imprinted bis-aniline-cross-linked AuNPs matrix in the absence of TNT is ∼200 S·cm^{-1}, and upon the association of 50 fM TNT with the matrix, the conductivity changes by ∼10%, Figure 7. This conductivity change may then lead to successful ultrasensitive detection of TNT by the AuNPs composite. That is, at a TNT concentration of 50 fM, and according to eq 4, and the derived values of the association constants, we estimate that ∼17% of the binding sites are occupied by TNT molecules. Although very few recognition events occur in the matrix, the electronic perturbations at the interparticle bis-aniline bridges translate into a collective conductivity change of the whole composite. Presumably, the localized charge transfer between the π-donor and

acceptor units alters the dielectric function and therefore the conductivity of the interconnected nanoparticle composite, resulting in the SPR curve changes.[37]

It should be noted that recent measurements for the truly metallic state of polyaniline reported conductivities in the order of 10³ S·cm^{-1}, in accordance with the predictions of the Drude theory.[38] Also, the electrical conductivity of thin π-conjugated polymer layers was recently evaluated by SPR,[39] and a value of 600 S·cm^{-1} was estimated, which is in a good agreement with the experimental value of 500 S·cm^{-1}, measured by the widely used Van der Pauw method. These results support our conclusion that the ultrasensitive, label-free, SPR method for analyzing TNT originates, indeed, from conductivity changes within the bis-aniline-cross-linked AuNP matrix, as a result of the association of TNT. It should be noted that in a recent STM study[40] regarding the formation of a donor−acceptor complex between tetracyanoethylene (acceptor) and a monolayer of a tetramethyl xylyl dithiol (donor), a 50-fold increase in the conductivity through the monolayer was observed upon the formation of the complex, consistent with our analysis.

In order to highlight the importance of the present label-free SPR method for the detection of TNT, we decided to compare the sensitivity of our method (detection limit ∼1.2 × 10^{-3} ppt) to other reported TNT detection methods, Table 2. We found that our method is at least 10³-fold more sensitive than any of the previously reported methods.

Conclusions

A bis-aniline-cross-linked AuNPs composite synthesized on a Au surface by an electropolymerization process was introduced as an active matrix for the amplified surface plasmon resonance (SPR) detection of trinitrotoluene, TNT. The formation of π-donor−acceptor complexes between the π-donor bis-aniline units and the TNT electron-acceptor units alters the dielectric properties of the matrix, thus enabling the amplified SPR detection of the TNT analyte by following the SPR reflectance changes originating from the coupling of the localized NPs plasmon with the surface plasmon wave associated with the Au surface. We found that the association constant of TNT to the bis-aniline units is 3.9 × 10⁹ M^{-1} and defined the detection limit for the analysis of TNT by the composite to be 10 pM. The significance of the existence of the π-donor−acceptor complex for analyzing TNT was demonstrated by eliminating

(36) Jackson, J. D. *Classical Electrodynamics*, 2nd ed.; John Wiley & Sons: New York, 1975.

(37) (a) Georgiadis, R.; Peterlinz, K. A.; Rahn, J. R.; Peterson, A. W.; Grassi, J. H. *Langmuir* **2000**, *16*, 6759–6762. (b) Chegel, V. I.; Raitman, O. A.; Lioubashevski, O.; Shirshov, Y.; Katz, E; Willner, I. *Adv. Mater.* **2002**, *14*, 1549–1553.
(38) Lee, K.; Cho, S.; Park, S. H.; Heeger, A. J.; Lee, C.-W.; Lee, S.-H. *Nature (London)* **2006**, *441*, 65–68.
(39) Hur, Y.; Jin, S.; Gal, Y.; Kim, J.; Kim, S.; Koh, K. *Mol. Cryst. Liq. Cryst.* **2002**, *377*, 217–220.
(40) Kasibhatla, B. S. T.; Labonte, A. P.; Zahid, F.; Reifenberger, R. G.; Datta, S.; Kubiak, C. P. *J. Phys. Chem. B* **2003**, *107*, 12378–12382.
(41) Wang, J.; Bhada, R. K.; Lu, J.; MacDonald, D. *Anal. Chim. Acta* **1998**, *361*, 85–91.
(42) Zhang, H.-X.; Hu, J.-S.; Yan, C.-J.; Jiang, L.; Wan, L.-J. *Phys. Chem. Chem. Phys.* **2006**, *8*, 3567–3572.
(43) Hrapovic, S.; Majid, E.; Liu, Y.; Male, K.; Luong, J. H. T. *Anal. Chem.* **2006**, *78*, 5504–5512.
(44) Wang, J.; Hocevar, S. B.; Ogorevc, B. *Electrochem. Commun.* **2004**, *6*, 176–179.
(45) Mizuta, Y.; Onodera, T.; Singh, P.; Matsumoto, K.; Miura, N.; Toko, K. *Biosens. Bioelectron.* **2008**, *24*, 191–197.
(46) Singh, P.; Onodera, T.; Mizuta, Y.; Matsumoto, K.; Miura, N.; Toko, K. *Sens. Mater.* **2007**, *19*, 261–273.
(47) Shankaran, D. R.; Kawaguchi, T.; Kim, S. J.; Matsumoto, K.; Toko, K.; Miura, N. *Anal. Bioanal. Chem.* **2006**, *386*, 1313–1320.

Table 2. Comparison of different TNT sensors.

detection method	detection limit	reference
remote microelectrode electrochemical sensor in water	50 ppb	41
luminiscent oligo(tetraphenyl)silole nanoparticles in water	20 ppb	18
quenching of fluorescence of polymer films in air	10 ppb	16
electrochemical detection by carbon nanotubes in water	5 ppb	42
biochip (on Au) via QCM or SPR in water	$1-10$ ppb	25
electrochemical detection using metallic NP-CNT composites in water	1 ppb	43
adsorptive stripping by carbon nanotubes-modified GCE in water	600 ppt	44
electrochemical detection by mesoporous SiO_2-modified electrodes in water	414 ppt	20
oligo(ethylene glycol)-based SPR in water	80 ppt	45
electrochemical sensing by imprinted electropolymerized bis-aniline-cross-linked AuNPs in water	46 ppt	28
SPR, fabricated dinitrophenylated-keyhole lympet hemocyanin (DNP-KLH) protein conjugate (in water)	5 ppt	46
indirect competitive immunoassay using SPR (in water)	2 ppt	47
SPR sensing by bis-aniline-cross-linked picric acid-imprinted Au-nanoparticles composite	1.2×10^{-3} ppt	present study

the formation of the complex through the potential-induced transformation of the bis-aniline π-donor units into their quinoide electron-acceptor state.

We further advanced the analysis of TNT by introducing the imprinting process, whereby the electropolymerization of the bis-aniline-cross-linked composite was performed in the presence of picric acid, as a TNT analogue. The imprinted bis-aniline AuNPs composite revealed a two-step response that included an ultrasensitive analysis region in which TNT was detected at a limit of 10 fM, and is attributed to the analysis of TNT by the high-affinity imprinted association sites ($K_{ass.}^{I} = 6.4 \times 10^{12}$ M^{-1}). The second detection region was observed in the 10^{-10} M TNT range and is attributed to the association of TNT by the nonimprinted bis-aniline π-donor sites ($K_{ass.}^{NI} = 3.9 \times 10^{9}$ M^{-1}). The imprinted AuNPs matrix revealed impressive selectivity toward the analysis of TNT.

The ultrasensitive detection of TNT by SPR spectroscopy using the imprinted bis-aniline AuNPs composite is, to the best of our knowledge, the most sensitive and specific sensing interface for the TNT explosive. The resulting sensitivity of the AuNPs composite and its stability (over two months with no noticeable degradation), demonstrate the potential future applicability of the method, (i.e., detection of TNT in mine fields). Furthermore, the sensing matrices could be regenerated by rinsing off the associated TNT with a buffer solution (the matrices were reused five times without noticeable effect on their performance). Besides the analytical value of this research, the study tried to address the origin for the observed sensitivity, and to explain how a few recognition events can induce a readable reflectance change in the SPR spectra. The theoretical fitting of the experimental SPR curves, measured in the presence of variable concentrations of TNT, allowed us to follow the dielectric properties of the composite. We find that the changes in the dielectric properties of the matrix, as a result of a few charge transfer events at the donor−acceptor recognition sites, are translated into a collective measurable phenomenon, namely, a change in the dielectric function and conductivity of the AuNPs matrix.

Experimental Section

Nanoparticles Synthesis. Au nanoparticles (AuNPs) functionalized with 2-mercaptoethane sulfonic acid and *p*-aminothiophenol were prepared by mixing a 10 mL solution containing 197 mg of $HAuCl_4$ in ethanol, and a 5 mL solution containing 42 mg of mercaptoethane sulfonate and 8 mg of *p*-aminothiophenol in

methanol. The two solutions were stirred in the presence of 2.5 mL of glacial acetic acid on an ice bath for 1 h. Subsequently, 7.5 mL of aqueous solution of 1 M sodium borohydride, $NaBH_4$, was added dropwise, resulting in a dark colored solution associated with the presence of the AuNPs. The solution was stirred for one additional hour in an ice bath, and then, for 14 h at room temperature. The particles were successively washed and centrifuged (twice in each solvent) with methanol, ethanol, and diethyl ether. A mean particle size of 3.5 nm was estimated using TEM.

Chemical Modification of the Electrodes. *p*-Aminothiophenol-functionalized electrodes were prepared by immersing the Au slides for 24 h into a *p*-aminothiophenol ethanolic solution, 50 mM. In order to prepare the bis-aniline-cross-linked AuNPs composite on the electrode, the surface-tethered *p*-aminothiophenol groups were electropolymerized in a 0.1 M HEPES buffer solution (pH = 7.2) containing 1 mg·mL^{-1} of *p*-aminothiophenol-functionalized AuNPs. The polymerization was performed by the application of 10 potential cycles between −0.35 and 0.8 V vs Ag wire quasi-reference electrode, at a potential scan rate of 100 mV s^{-1}, followed by applying a fixed potential of 0.8 V for 30 min. The resulting films were, then, washed with the background buffer solution to exclude any residual monomer from the electrode. Similarly, picric acid-imprinted oligoaniline-cross-linked films were prepared by adding 1 mg·mL^{-1} picric acid to the AuNPs mixture prior to the electropolymerization process. The extraction of the picric acid from the film was carried out by immersing the electrodes in a 0.1 M HEPES solution, pH = 7.2, for 2 h at room temperature. The full removal of picric acid from the electropolymerized film was verified electrochemically. In a control experiment, a two-layer AuNPs matrix was assembled on the Au-coated glass surface by the primary association of thiopropionic acid-stabilized AuNPs (diameter 3.5 nm) on the cystamine-monolayer-functionalized gold slide, followed by the assembly of a second AuNPs layer by cross-linking the second layer of AuNPs to the base AuNPs layer using 1,4-butane dithiol.

Instrumentation. A surface plasmon resonance (SPR) Kretschmann type spectrometer NanoSPR 321 (NanoSPR devices, USA), with a LED light source, λ = 650 nm, and with a prism refraction index of *n* = 1.61, was used in this work. The SPR sensograms (time-dependent reflectance changes at a constant angle) represent real-time changes, and these were measured *in situ* using a home-built fluid cell. Au-coated semitransparent glass slides (Mivitec GmbH, Analytical μ-Systems, Germany) were used for the SPR measurements. Prior to modification, the Au surface was cleaned in hot ethanol, at 60 °C, for 30 min. For the electrochemical polymerization and SPR measurements employing *in situ* constant potential application, an auxiliary Pt (0.5 mm diameter wire) and a quasi-reversible reference Ag electrode (QRE) (0.5 mm diameter wire) were installed into a Perspex cell (volume 0.5 cm^3, working area

0.4 cm^2). For the constant potential measurements the SPR electrode potential was biased (vs Ag QRE), and the respective SPR curve was recorded in the presence of 100 fM TNT. For these measurements an Autolab electrochemical system (Echo Chemie, The Netherlands) driven by GPES software was used. The error bars presented for the different measurements correspond to $N = 5$ experiments. Atomic force microscopy (AFM) images were captured in a tapping mode on a Digital Nanoscope IV instrument employing Si cantilevers (NSC15/AIBS, MicroMash, Estonia, resonance frequency order of 320 kHz). Ellipsometry measurements were performed with a Woollam M-88 spectroscopic ellipsometer equipped with the WVASE 32 software.

Fitting of Experimental Results. Fresnel's equation-based SPR modeling for a five-layer system was performed using Winspall 2.0 program, generously provided by Prof. W. Knoll (Max Planck Institute for Polymer Research in Mainz, Germany. Present address: Austrian Research Centers GmbH Donau-City-Strasse 1, 1220 Vienna, Austria). A refractive index for bulk Au, $n = 0.173 + 3.422i$, was used for the modeling as the refractive index for the AuNPs. The Langmuir isotherm fittings were performed using Origin 7.5 software (Origin Laboratory Corporation).

Supporting Information Available: The AFM topography image of the bis-aniline-cross-linked AuNPs composite. This material is available free of charge via the Internet at http://pubs.acs.org.

JA9001212